A Pliocene mega-tsunami deposit and associated features in the Ranquil Formation, southern Chile

J.P. Le Roux [a,*], Sven N. Nielsen [b,1], Helga Kemnitz [b], Álvaro Henriquez [a]

[a] *Departamento de Geología, Facultad de Ciencias Físicas y Matemáticas, Universidad de Chile, Casilla 13518, Correo 21, Santiago, Chile*
[b] *GeoForschungsZentrum Potsdam, Section 3.1, Telegrafenberg, 14473 Potsdam, Germany*

Abstract

An exceptionally large tsunami affected the coastline of southern Chile during the Pliocene. Its backflow eroded coarse beach and coastal dune sediments and redistributed them over the continental shelf and slope. Sandstone dykes and sills injected from the base of the resulting hyperconcentrated flow into underlying cohesive muds, assisted in plucking up large blocks of the latter and incorporating them into the flow. Locally, the rip-up intraclasts were fragmented further by smaller-scale injections to form a distinct breccia of angular to rounded mudstone clasts within a medium to coarse sandstone matrix. Sandstone sills in places mimic normal sedimentary beds, complete with structures resembling inverse gradation, planar laminae, as well as ripple and trough cross-lamination. These were probably formed by internal sediment flow and shear stress as the semi-liquefied sand was forcefully injected into cracks. In borehole cores, such sills can easily be misinterpreted as normal sedimentary beds, which can have important implications for hydrocarbon exploration.

Keywords: Tsunami; Sandstone dykes; Debris flow; Mimic sedimentary structures; Eltanin impact; Hydrocarbon reservoirs

1. Introduction

The west coast of South America has a narrow shelf and steep continental slope into a deep subduction trench. It is seismically one of the most active regions in the world (Kulikov et al., 2005) and tectonism triggering large-magnitude earthquakes produces fairly regular near-field tsunami events. Furthermore, the coastline is also swept from time to time by far-field tsunamis from elsewhere in the Pacific Ocean, both as a result of tectonic processes and bolide impacts. In Chile, these events are reflected in the geological record by Neogene deposits interpreted as ancient debris flows with associated sedimentological features including large rip-up clasts and well rounded basement boulders incorporated into the debris, as well as sand injection from the base of the flows into the substrate (Paskoff, 1991; Hartley et al., 2001; Cantalamessa and Di Celma, 2005; Le Roux et al., 2004; Le Roux and Vargas, 2005).

A submarine debris flow deposit at Ranquil south of Concepción (Fig. 1), mentioned by Le Roux and Vargas (2005) as representing a possible tsunami bed but not described in any detail, was investigated to try and determine its age and origin. The deposit differs from other debris flow beds along the Chilean coastline, which are generally composed of poorly sorted, coarse conglomerate or coquina with large basement boulders, by its finer texture (medium to very coarse sandstone), the presence of mudstone-clast breccia, and unusually large dykes and sills penetrating the substrate. Because the sandstone is generally massive, interpretation of its origin based on sedimentary structures is not feasible, so that its grain surface textures were studied instead.

* Corresponding author. Tel.: +56 2 9784123.
E-mail address: jroux@cec.uchile.cl (J.P. Le Roux).
[1] Current address: Institut für Geowissenschaften, Christian-Albrechts-Universität Kiel, Ludewig-Meyn-Str. 10, 24118 Kiel, Germany.

2. Geological background

Neogene successions reflecting continental to continental slope environments occur in several isolated basins along the Chilean coast between Antofagasta and the Taitao Peninsula (Fig. 1). These have been described in several publications (e.g. Le Roux and Elgueta, 1997, 2000; Le Roux et al., 2004, 2005a,b, 2006; Encinas et al., 2006a,b). Here we focus on the Huenteguapi sandstone, which forms part of the Ranquil Formation of the Arauco Basin extending south from Concepción (Figs. 1 and 2). Deposits within this basin range from the Cretaceous to the Neogene, with eight formations overlying the Paleozoic metamorphic basement and in turn overlain by Holocene sediments (Table 1). Deposition took place in continental to shallow marine, shelf and continental slope environments, with coal beds occurring in the Curanilahue and Trihueco Formations (Pineda, 1986; Le Roux and Elgueta, 1997; Schöning and Bandel, 2004).

The Ranquil Formation as defined by García (1968) has an unconformable contact with the underlying Lebu Group (Millonhue Formation) of Paleogene age and is unconformably overlain by the upper Pliocene to lower Pleistocene Tubul Formation (Martínez, 1976; Schöning and Bandel, 2004; own unpublished data). The concurrent range of several planktic foraminifers including *Globoquadrina dehiscens* (N4b–N17/N19a), *Globorotalia spheriomiozea* (N17–N19a), and *Globorotalia puncticulata* (N19–N21) indicates a late Miocene (Tortonian) to early Pliocene (Zanclean) age for the lower members of the Ranquil Formation (Finger et al., 2007), which underlie the Huenteguapi sandstone. A calcareous sandstone bed (RQK of Finger et al., 2007) overlying the latter has a Zanclean to Gelasian age (5.3–1.8 Ma) as shown by the presence of the planktic foraminifers *Globigerinella obesa* s.l. (since P22), *Orbulina universa* (since N9) and *G. puncticulata* (N19–N21) (Finger et al., 2007). The Huenteguapi sandstone therefore probably has a Zanclean to Gelasian age (5.3–1.8 Ma), although no age diagnostic planktic foraminifers were recovered from this bed.

The stratigraphy of the Ranquil Formation is shown in Fig. 3. It commences with a basal unit (U1) of interbedded fine sandstone and shale, overlain by matrix-supported conglomerate with fine sandstone and siltstone clasts in a clayey to silty matrix (U2). This is succeeded by grey mudstones intercalated with fine, calcareous sandstones showing parallel lamination, ripple and hummocky cross-lamination, as well as slump and fluid escape structures (U3). Schöning and Bandel (2004) identified ten dicotyledonous tree families in silicified wood fragments collected from this unit, all of which indicate a humid climate. Le Roux et al. (submitted for publication) considered unit U3 to reflect a continental shelf environment on the basis of its sedimentary facies, benthic foraminifers including *Hansenisca soldani*, *Pyrgo depressa*, *Sphaeroidina bulloides* and *Nodogenerina sagrinensis* (Finger et al., 2007), as well as a trace fossil suite including *Zoophycos*, *Chondrites*, *Phycosiphon*, *Nereites missouriensis*, *Lackeia siliquaria*, *Psammichnites*, *Parataenidium*, *Ophiomorpha* and *Rhizocorallium*. Flute marks at the base of some sandstone beds suggest occasional turbidity currents.

The upper part of this succession is formed by light green, massive mudstones and laminated shales with rare interbedded,

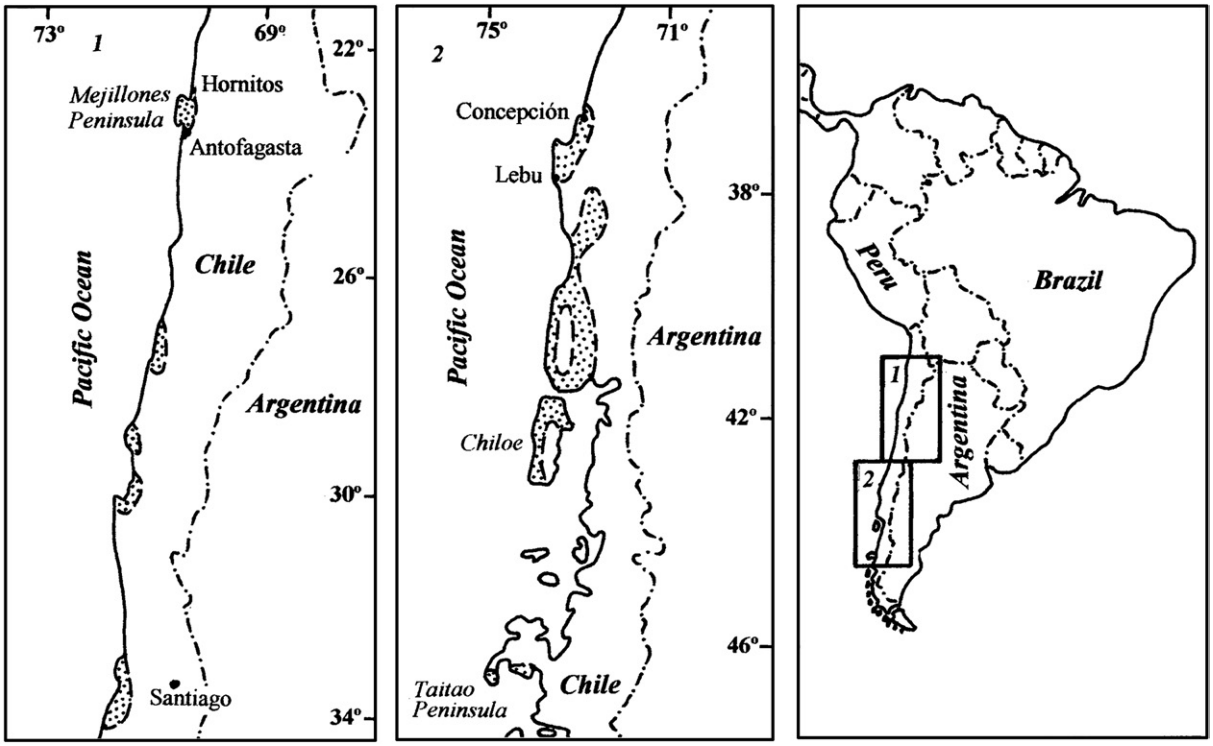

Fig. 1. Distribution of Neogene marine basins in Chile.

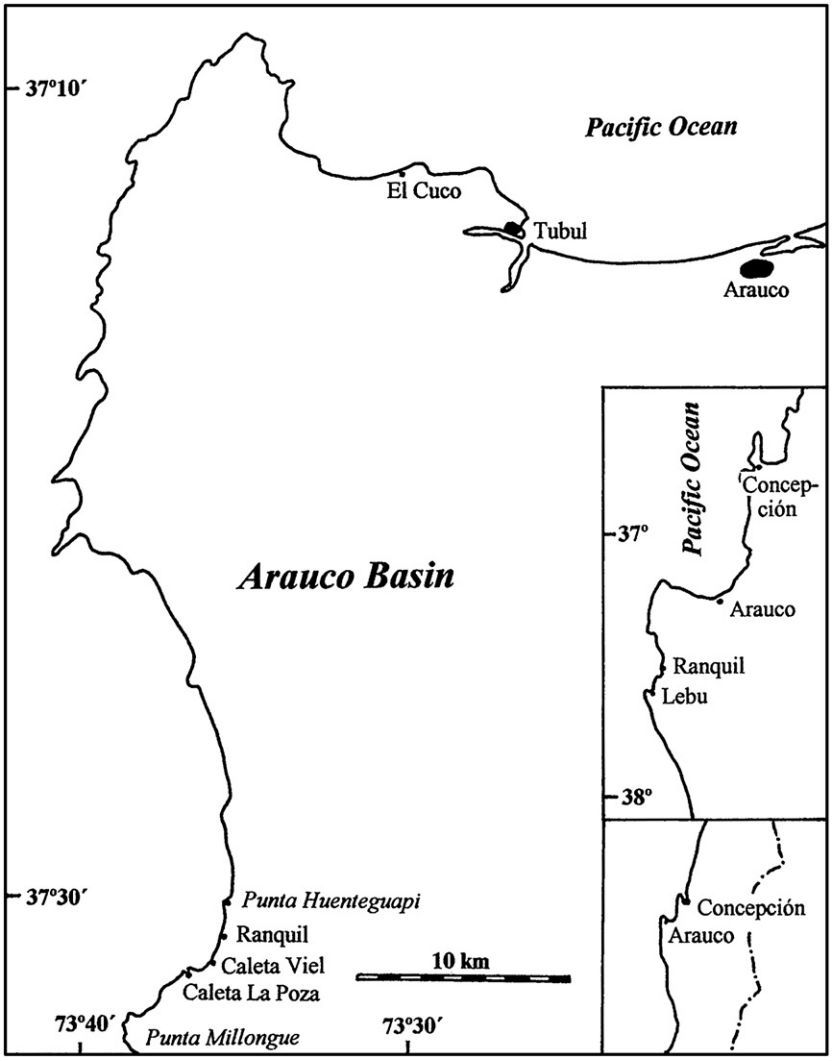

Fig. 2. Locality map of Arauco Basin showing places mentioned in text.

fining-upward sandstones. The latter are 70–150 cm thick and very fine-grained with occasional flute structures at the base. They show planar lamination grading upward into small-scale trough or ripple cross-lamination, thus resembling partial Bouma cycles. Slump and fluid escape structures are locally present. The gastropods *Olivancillaria claneophila* (Nielsen, 2004), *Sinum subglobosus* and *Diloma miocenica*, which are also present in the lower members of the Ranquil Formation, occur within this unit (Nielsen et al., 2004). Within the mudrocks are also large sinuous, branched burrows of *Thalassinoides*, together with *Zoophycos* and *Chondrites* traces typical of a bathyal environment (Buatois et al., 2002) and calcareous concretions containing the trace fossil *Stelloglyphus* (Le Roux et al., submitted for publication). Benthic foraminifera and psychrospheric ostracodes, e.g. *Krithe* spp., also indicate a bathyal depositional depth of about 2000 m for the upper part of this unit (Finger et al., 2007). Duranti and Hurst (2004) attributed similar successions with *Thalassinoides* burrows as hemipelagic deposits interbedded with low-density turbidites.

In some areas massive, fine sandstones with thin interbeds of bioturbated, medium sandstone and conglomerate are present (U4) at the top of the succession beneath the Huenteguapi sandstone. However, the latter generally overlies unit U3 directly.

Table 1
Stratigraphy of depositional units in the Arauco Basin, after Pineda (1986)

Dunes, etc.	Holocene (<0.01 Ma)
Tubul Formation	Upper Pliocene–lower Pleistocene (2.6–0.8 Ma)
Ranquil Formation	Tortonian–Gelasian (11.6–1.8 Ma)
Lebu Group	
Millonhue Formation	Bartonian–Priabonian (upper Eocene) (40.4–33.9 Ma)
Trihueco Formation	Lutetian (lower Eocene) (48.6–40.4 Ma)
Boca Lebu Formation	Ypresian (lower Eocene) (55.8–48.6 Ma)
Curanilahue Formation	
Pilpilco Formation	Paleocene–lower Eocene (65.5–40.4 Ma)
Quiriquina Formation	Maastrichtian (Upper Cretaceous) (70.6–65.5 Ma)
Paleozoic Basement	

Ages according to International Stratigraphic Chart of the International Commission on Stratigraphy, 2004.

3. Description of the Huenteguapi sandstone and associated features

3.1. Huenteguapi sandstone

3.1.1. Field relationships

The Huenteguapi sandstone crops out locally over a distance of about 3 km between Caleta La Poza and Punta Huenteguapi (Fig. 2). Sandstone intrusions and mudstone-clast breccia that are directly associated with this unit also occur as far as El Cuco 40 km north of La Poza, but the bed is interrupted by faults or eroded in the areas in-between. However, no other similar, medium to very coarse sandstone unit is known from the Neogene in the Arauco Basin, so that it seems to be unique in a succession of fine to very fine-grained deposits reaching a total thickness of at least 500 m (including the overlying Tubul Formation; Pineda, 1983).

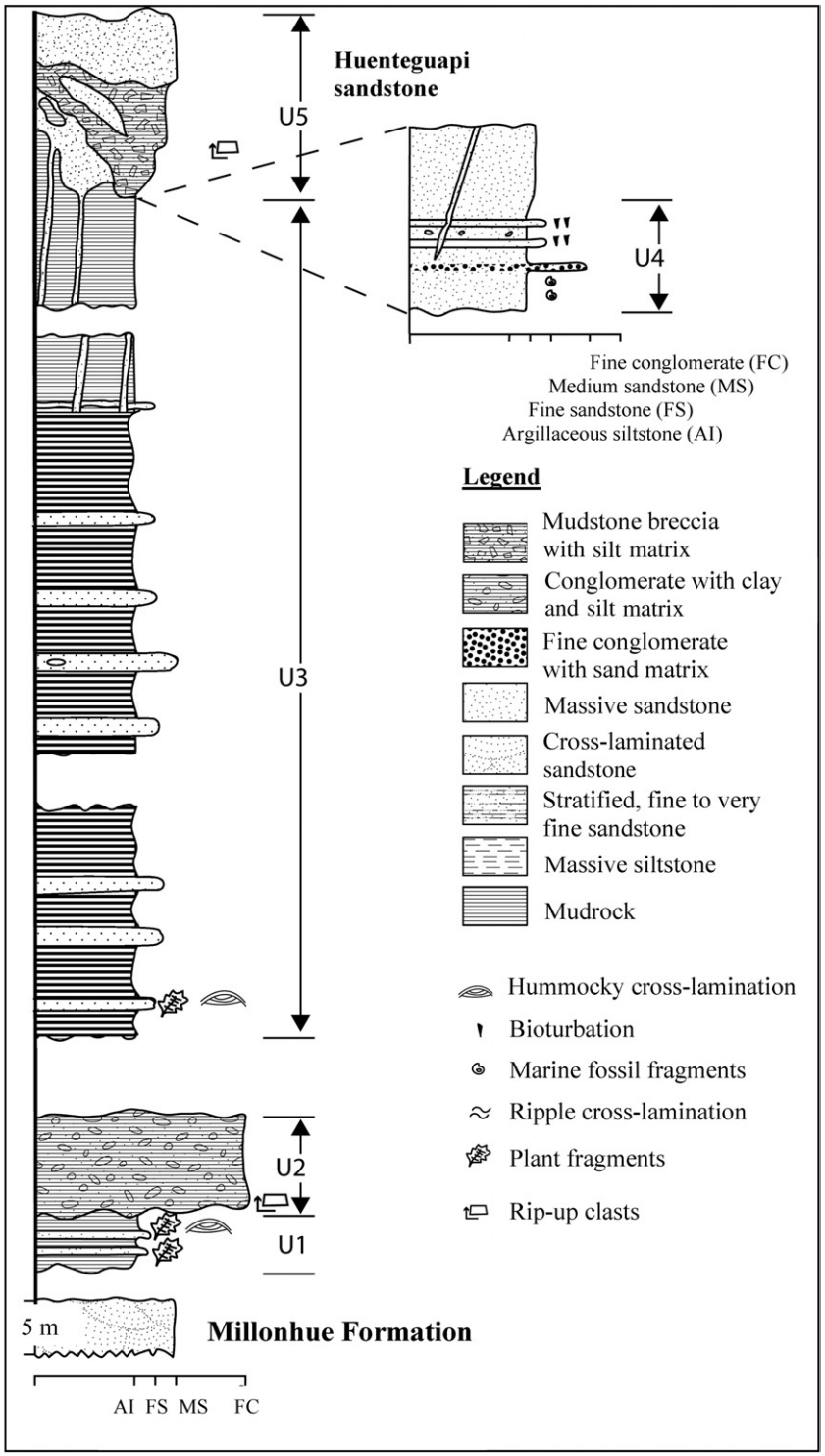

Fig. 3. Stratigraphy of the Ranquil Formation (after García, 1968; Henriquez, 2006).

The Huenteguapi sandstone has an exposed thickness of at least 5 to more than 30 m, but its maximum thickness is unknown. It has an eroded, very irregular basal contact with local channels exceeding 5 m in depth. The contact, especially along channel zones, is commonly displaced by small synsedimentary faults.

The unit is generally massive, consisting of medium to very coarse and poorly to very poorly sorted sandstone, locally grading into granules or small-pebble conglomerate. Floating mudstone clasts are common and locally served as nuclei for ferruginous concretions ranging in scale from a few cm to several tens of cm. They are locally concentrated along and oriented parallel to the channel base and steep channel margins. In some cases, the clasts along the basal contact show a clear coarsening-upward size-grading (Fig. 4).

3.1.2. Fossil content

A variety of shell fossils are present within the Huenteguapi sandstone itself, including *Nacella*, *Fissurella*, *Hipponix*, *Crassilabrum* and *Acanthina*, as well as barnacles (Nielsen, submitted for publication). These taxa are not known to occur in the lower members of the Ranquil Formation. No microfossils have so far been recovered from the sandstone itself, although rip-up mudstone clasts derived from the uppermost part of unit U3 contain bathyal foraminifers (Finger et al., 2007). Some rip-up clasts, e.g. at Punta Huenteguapi, also contain the gastropods *O. claneophila*, *S. subglobosus* and *D. miocenica* (Finger et al., 2007).

3.1.3. Quartz grain surface textures

3.1.3.1. Concept and methodology. During transport by various agents, processes such as collision and abrasion leave different types of erosional microfeatures on grain surfaces that are easily observable under a scanning electron microscope (SEM). Each of those microtextures is typical of a certain intensity, turbulence, and type of motion. Quartz, being both abundant in many source rocks and resistant to long distances of transport or periods of reworking, is therefore the most appropriate candidate for this kind of study.

To identify the processes that affected grain surfaces, it is necessary to establish characteristic microtexture groups (Krinsley and Donahue, 1968; Higgs, 1979; Bull, 1981), because similar conditions operating in different environments can generate a range of similar features (Brown, 1973). Statistical analysis (Culver et al., 1983) also showed that a combination of features should be used to distinguish different environments.

For statistical confidence, at least 30–40 grains per sample are required (Trewin, 1988); 54 grains were analyzed in this study. The examined quartz grains range from medium sand to fine gravel size (500–1000 μm), which guarantees that abundant abrasion and collision effects can be observed (Krischev and Georgiev, 1981).

After washing and sieving, the remaining fraction exceeding 250 μm was boiled in 18% hydrochloric acid for 20 min and dried in an oven overnight at 50 °C. Grains were then picked at random under a stereomicroscope, adjusted in rows on SEM stubs, and sputter-coated with gold-palladium. A number was allotted to each grain and recorded on an overlay on the SEM screen to allow easy tracking of individual grains. An additional micro-analytical check on the selected grains proved to be useful, as some of the milky-white grains turned out to be plagioclase (andesine), whereas some crystal-clear grains were glass. This examination and the quartz grain surface analysis were performed with a Zeiss SEM (DSM

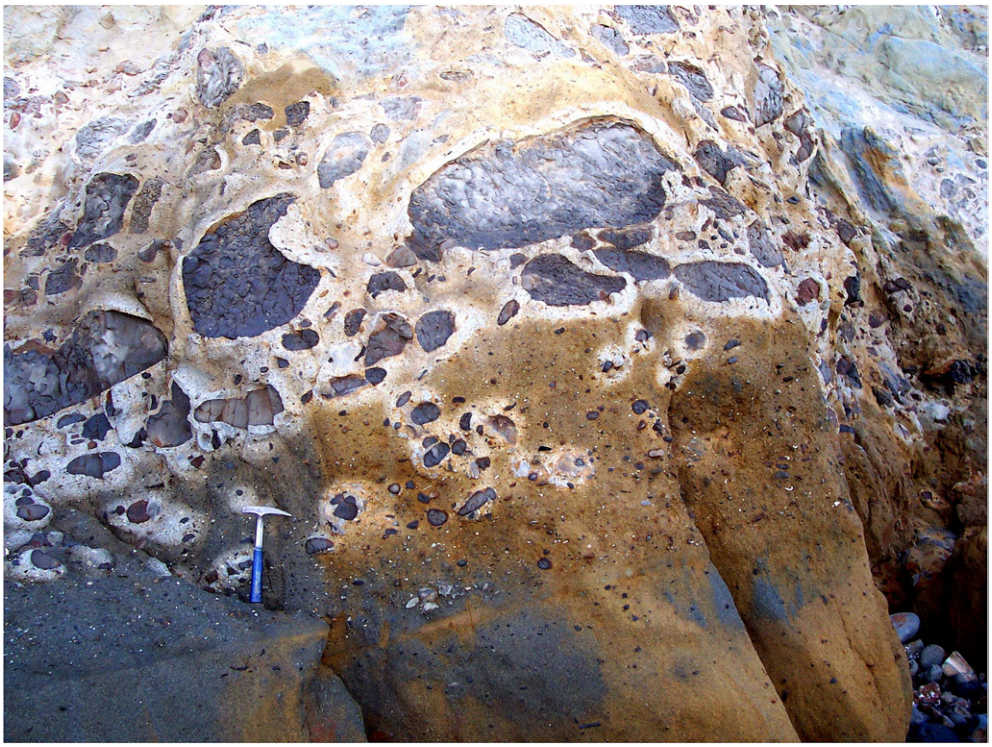

Fig. 4. Coarsening-upward zone of mudstone clasts at base of channel, indicating dispersive pressure because of shearing.

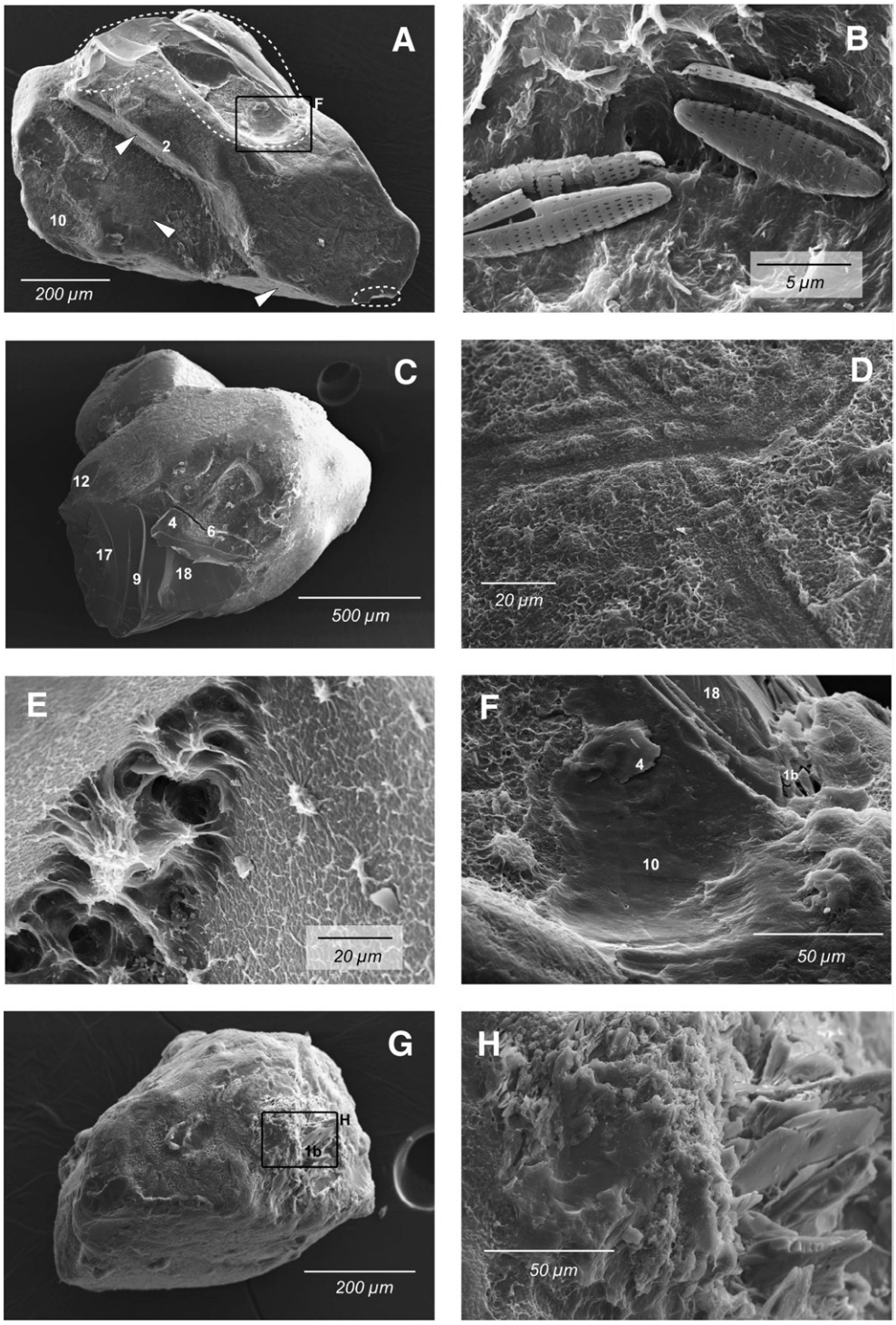

Fig. 5. (A) Oldest fracture planes (arrows), craters (10), and blocky structure (2) of Process I became smoothened by aeolian transport (Process II). Overgrowth with a siliceous web of an uncertain biogenic origin followed (Process III) and was eventually partly destroyed by Process IV (marked areas). (B) Poorly preserved diatoms in a solution pit, partly embedded in siliceous material. (C) Large collision features, high relief and a large uplifted block (4) on a bulbous, rounded grain (Process II) are associated with the high-energy event (Process IV). Image shows conchoidal (17) and radial fractures (18), deep step-like grooves (9), incisions (12), and cracks on edges (6). (D) Details of the former aeolian abraded surface are covered by a siliceous web of unknown origin. Center shows criss-crossing imprints of possible biogenic origin (algae?). (E) Etch structures of organic origin(?) associated with Process III. (F) Detail of (A) shows a high-energy impact crater (10) and fracture features (background) of medium size (18), and shattering effects (1b, 4; Process IV) erasing the siliceous web structure linked to Process III. (G) Surface with shatter structure (1b; Process IV). (H) Detail of (G) shows small to large plates and blocks upturned into a position orthogonal to the surface of the grain (Process IV).

962) equipped with an energy-dispersive system and a NORVAR Si–Li detector (Thermo Fisher Scientific) at 20 kV acceleration voltage.

As a next step, both shape features (stereomicroscope) and surface microfeatures (SEM) were documented. The SEM study also included visual estimation and documentation of the relative

frequency or intensity (in percentage) of the microfeatures on each grain. This assisted in the subsequent comparison of different samples and sample environments and to distinguish between texture groups developed in similar environments, but under different energy intensities. In addition, the age relationships between features based on indications of textural superposition were included in this record. When these clearly proved to form age-dependent feature groups and to follow the same temporal succession, they were documented separately on a working sheet representing a certain process or event.

3.1.3.2. Characteristic microtextures and feature groups. Four distinct microtextural groups characterize the quartz grains of the sample from the Huenteguapi sandstone (Fig. 5).

The oldest features (Process I), present on about 90% of all 54 grains, comprise a wide range of high to intermediate energy marks of medium to large size. These are predominantly edge abrasion, V-shaped pits and incisions of different sizes, large blocks, grooves and craters, and crescent-shaped gouge marks (Fig. 5A). Adhering diatoms can be observed on approximately 10% of these grains. Like the other textures of this group, the diatoms are often covered by precipitated silica or partially destroyed by younger surface abrasion and impact marks (Fig. 5B).

The second process (II) is represented on 93% of all grains, which show rounded and bulbous edges, V-shaped pits in series covering the abraded surface and other impact marks always ranging on a scale of 2–20 μm (Fig. 5A, C). Most of the abraded surface areas show rows of very small uplifted plates, partly smoothed over by silica precipitation and resulting in a so-called orange peel appearance.

The third textural group (Process III) shows etching pits on the surface of about 35% of the grains. Webs of probable

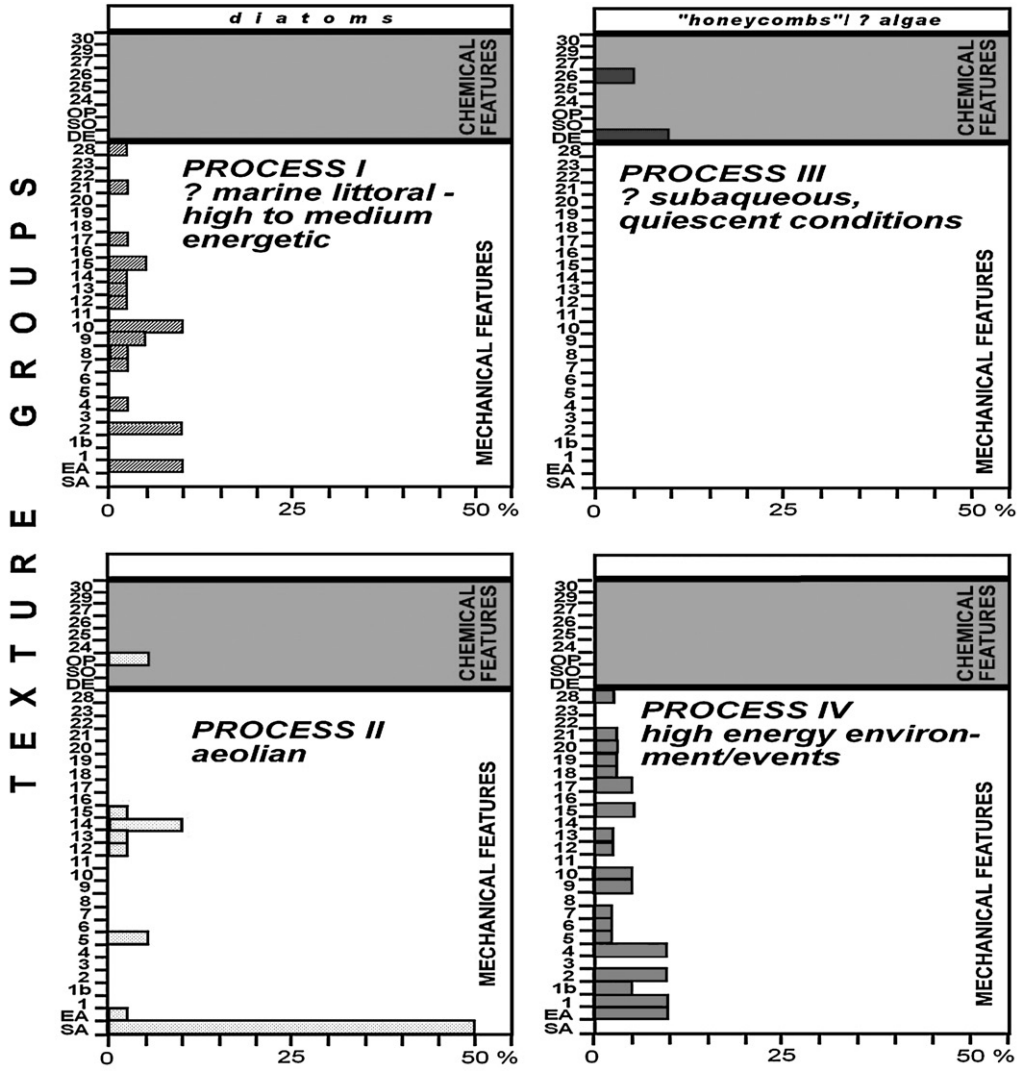

Fig. 6. Comparison of microtexture group patterns and frequencies of single surface features. SA — surface abrasion; EA — edge abrasion; 1 — small blocks; 1b — shatter structure; 2 — large blocks; 3 — imbricated blocks; 4 — large uplifted plates; 5 — small uplifted plates; 6 — cracks on edges; 7 — linear grooves; 8 — curved grooves; 9 — deep grooves; 10 — craters; 11 — striation; 12 — V-shaped incisions; 13 — V-shaped pits, random and different sizes; 14 — V-shaped pits in series; 15 — crescent-shaped gouges; 16 — small conchoidal fractures; 17 — large conchoidal fractures; 18 — radial fractures; 20 — parallel steps; 21 – curved steps; 22 — ridges; 23 — sawtooth structures; DE — dissolution etching; SO — silica overgrowth; OP — orange peel; 24 — silica globules; 25 — crystal growth; 26 — solution pits; 27 — crystallographically oriented etched pits; 28 — cracks, irregular; 29 — polygonal cracks; 30 — etched grooves.

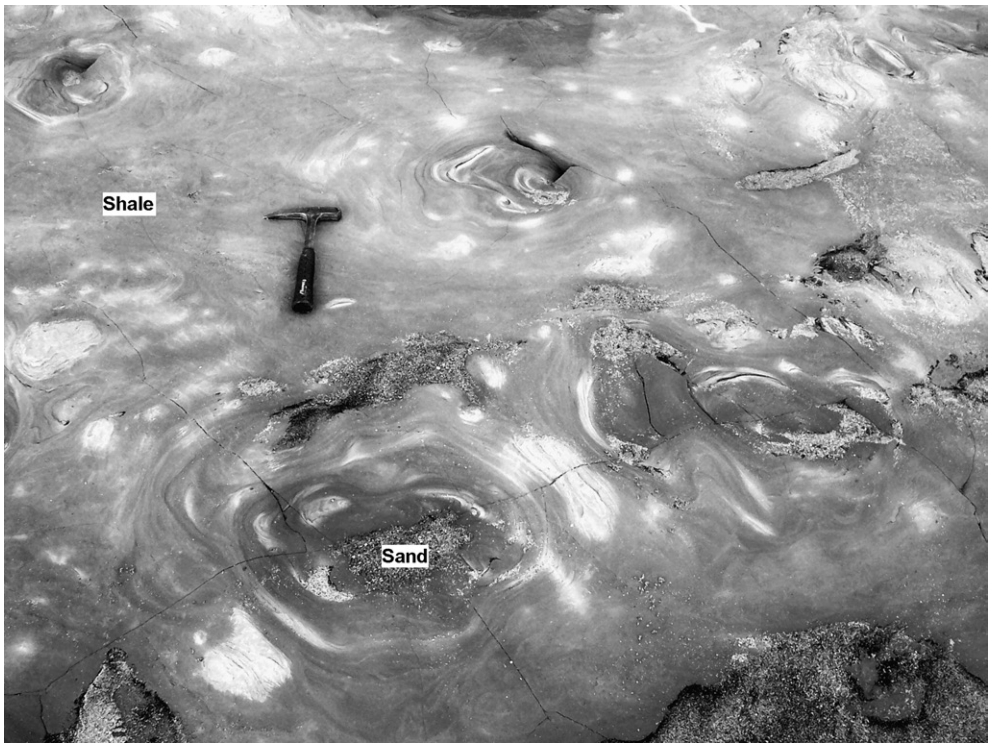

Fig. 7. Ring structures with sandy cores in shales underlying the Huenteguapi sandstone. These are interpreted as upward fluid escape pipes, because the laminae are bent upward around the cores.

biogenic origin, possibly colonies of algae, partly cover large parts of the grains. In addition, some rare prints of algae(?) also seem to belong to this third stage of the sedimentation history (Fig. 5D). However, interpretation of the siliceous web material as of being biogenic origin has not been proven (Fig. 5E).

The fourth and youngest grain surface features (Process IV) are represented by fresh breakage faces and large, communicating,

Fig. 8. Ring structures in shales underlying Huenteguapi sandstone, accentuated by *Thalassinoides* concentrated in a bed that was subsequently updomed by fluid escape.

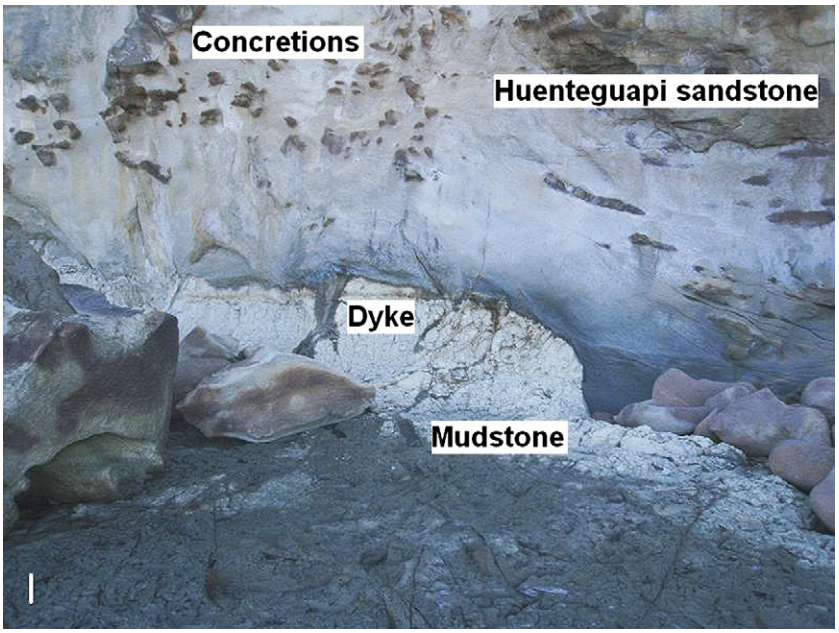

Fig. 9. Sandstone dyke emanating from base of Huenteguapi sandstone. White line at bottom left represents 30 cm.

conchoidal, radial, and step-like fractures (Fig. 5A, C, F). They partially destroyed all the older features including the possible algae web. To a different degree these textures affect all grains of the sample, although they are generally not abundant. Some additional, very special features also distinguish this group from others: Shatter structures consist of upright plates of different size (10–50 μm), here described under the category of "small plates" (Fig. 5G, H; Fig. 6). Also typical, but more rare are cracks on edges. Furthermore, some grains show an apparent local effect of silica melting.

Fig. 10. Sandstone dyke penetrating large mudstone rip-up clast within the Huenteguapi sandstone from below. Note sinuous shape of dyke (due to compaction) and lamination parallel to dyke walls. The ferruginous concretions in the lower left part of the photo formed around mudstone clasts.

Fig. 11. Dykes and sills at Caleta Viel (Fig. 2). Geological hammer in rectangle is about 30 cm long.

3.2. Description of associated features

3.2.1. Ring-shaped structures

A prominent feature observed in the shales (U3) immediately underlying the Huenteguapi sandstone are circular structures (Fig. 7) with laminae bent upward around sandy cores. The bedding is in some cases accentuated by calcareous concretions or *Thalassinoides* burrows (Fig. 8). These structures reach a maximum diameter of 4–5 m and occur some meters below the Huenteguapi sandstone. They apparently formed by updoming

Fig. 12. Oblique dyke cutting across bedding shown by siltstone beds in mudstone unit. Mimic sedimentary structures and bedding (Figs. 13, 14) occur in this unit.

Fig. 13. Laminae of coarser and finer sandstone in oblique dyke (Fig. 12) caused by shearing during intrusion. Note concentration of clasts in some layers. Lamination was probably produced by shear during sill intrusion.

or breaching of beds rich in concretions and nodules or intensively burrowed by *Thalassinoides*.

3.2.2. Sandstone intrusions

Intrusions emanating from the base of the Huenteguapi sandstone (Fig. 9) range in scale from a few mm to more than 2 m wide (Fig. 10), and a few cm to more than 30 m in length. Their orientations vary from near-vertical and oblique to horizontal, parallel to the bedding. Many of the larger dykes and sills split up into smaller veins, often at right angles to the main intrusions. Such criss-crossing dykes and sills commonly occur in zones exceeding 30 m in thickness, as for example at Punta Huenteguapi and Caleta Viel (Fig. 11). At the latter locality, for example, a sandstone sill mimics a normal sandstone bed but shows veins protruding both up and down into the surrounding mudstone. These secondary veins are on average about 4 cm wide and reach more than 5 m in length. They are locally irregular to sinuous in shape, probably as a result of compaction, with well developed pinch-and-swell structures. Further south this sill changes into an oblique dyke that cuts across the bedding, here revealed by thin siltstone interbeds within the mudstone (Fig. 12).

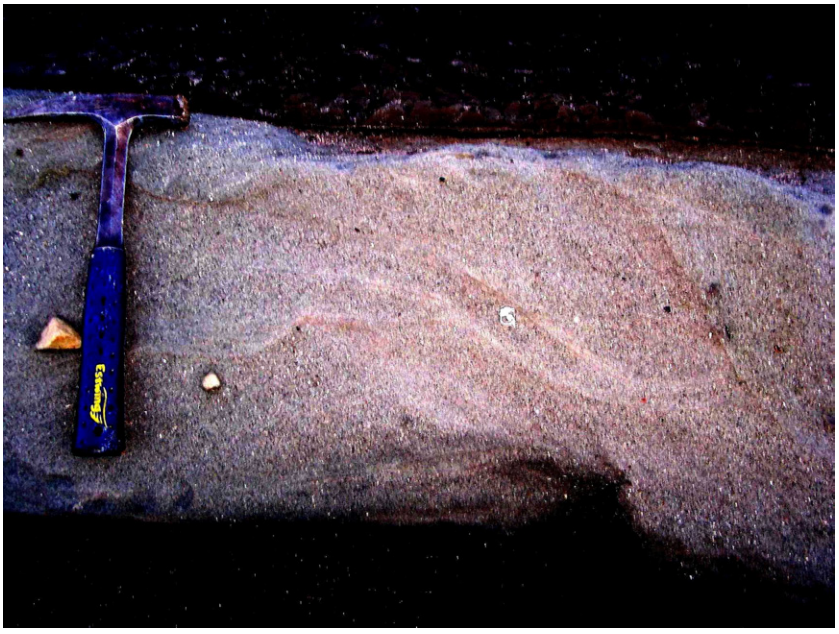

Fig. 14. Mimic trough cross-lamination in oblique sandstone dyke (Fig. 12).

Fig. 15. Large mudstone clast within Huenteguapi sandstone. Ferruginous concretions formed around smaller clasts.

The dykes and sills are generally finer-grained than the source bed at the same locality. An outcrop north of Ranquil, for example, shows well developed lamination formed by coarse to granular sandstone at the base of the Huenteguapi sandstone. A few tens of cm higher up, this coarse sandstone is eroded by medium sandstone along a smoothly undulating contact showing up to 50 cm relief. Locally, the medium sandstone protrudes through the coarse sandstone into the underlying mudstone, where it forms small dykes.

Although the sandstone within the intrusions is generally massive, it locally shows well developed vertical lamination parallel to the sides of the dykes. These laminae assume a horizontal orientation where the dykes pass upward or downward into sills. In other cases, for example at Caleta Viel,

Fig. 16. Mudstone-clast breccia formed by multiple injections breaking up large rip-up clasts. The rounded clasts in the photo probably formed earlier than angular clasts and were reshaped within the flow.

sandstone sills display laminae of fine, medium and coarse sandstone (Fig. 13) that locally mimic ripple and trough cross-lamination (Fig. 14). Mudstone clasts within the dykes and sills are also commonly oriented parallel to the walls of the intrusions, where they show inverse size-grading similar to that observed at the base of the Huenteguapi sandstone.

3.2.3. Mudstone-clast breccia

Irregular inclusions and mega-inclusions of mudrock are common within the Huenteguapi sandstone (Fig. 15), in some cases reaching more than 5 m in diameter. Some of these mudstone clasts contain *Thalassinoides* traces. At many localities, for example east of El Cuco (Fig. 2), angular to well rounded mudstone, siltstone or fine sandstone clasts become so numerous within the Huenteguapi sandstone that they form a breccia with a medium to coarse sandstone matrix (Fig. 16).

4. Interpretation of the Huenteguapi sandstone and associated features

4.1. Huenteguapi sandstone

4.1.1. Field relationships

The generally massive nature of the Huenteguapi sandstone, together with many floating mud clasts indicative of hindered settling, is typical of sandy debris flow deposits (Shanmugam, 2000; Amy et al., 2005). A sandy debris flow origin is supported by the coarsening-upward zones of mudstone clasts along the channel base (Fig. 4), suggesting a strong shearing action (Todd, 1989). Although it can be argued that dense, laminar flows cannot produce erosion and steep-sided channels because of the absence of large-scale turbulence, in this case there is ample evidence that very large blocks of mudstone were plucked from the substrate, which partly explains this feature. Le Roux et al. (2004) also provided evidence that turbulent flows can form as a result of the large volumes of water displaced ahead of debris flows, which can erode the substrate and channelize the debris along certain zones.

Direct evidence for laminar flow is in this case provided by the orientation of smaller mudstone clasts parallel to the steep sides of channels. This not only indicates a strong shearing action higher up in the flow, but also that the flow was dense enough to prevent them from sinking to the bottom.

The presence of synsedimentary microfaults at the base of some channels may be either attributed to loading, produced by the sudden deposition of large volumes of sand in the depressions formed by preceding turbulent flows and plucking, or to post-depositional compaction.

4.1.2. Fossil content

The gastropods *O. claneophila*, *S. subglobosus* and *D. miocenica* recovered from mudrock rip-up clasts within the Huenteguapi sandstone, are typical of the early Miocene (Nielsen and Glodny, 2006). This indicates reworking of older beds not presently exposed in the study area, into the Ranquil Formation, from where they may have been reworked again into the Huenteguapi sandstone via rip-up clasts (Finger et al., 2007). Coastal erosion of rocky shorelines is also indicated by the presence of rocky coast gastropod genera *Nacella*, *Fissurella*, *Hipponix*, *Crassilabrum*, *Acanthina*, and barnacles which are not known from the underlying sandstone and mudstone beds. This strongly argues in favour of a debris flow originating along the coast and passing into the deeper water of the continental shelf and slope.

4.1.3. Quartz surface textures

To test the reliability of interpretations based on grain surface textures, abrasion mechanisms were experimentally simulated by Krinsley and Doornkamp (1973), Linde and Mycielska-Dowgiallo (1980), Wellendorf and Krinsley (1980), Krinsley and Wellendorf (1980), and Whalley et al. (1982) for different environments. Our interpretation of the observed texture groups is partly based on their findings, as well as reviews by Higgs (1979) and Bull (1981) on the relationships between these textures and depositional environments.

The first texture group (I) can most probably be linked to collisions in a subaqueous medium. The pattern of this texture group, although differing in intensity from grain to grain, best resembles a littoral environment (Higgs, 1979). This interpretation is supported by the adhering diatoms. Because the intensity of the single features vary, and as part of them apparently show a development from high- to low-energy feature groups with time, they may also reflect a longer multiple-phase process or even a decrease in hydrodynamic energy caused by changes in the coastline morphology. However, because of subsequent abrasion and chemical processes, the environmental interpretation of this group has the highest uncertainty among the identified processes.

The second texture group (II) is very typical of aeolian deposits. The common bulbous and rounded edges of the grains reflect spinning under aeolian transport conditions (Whalley and Marshall, 1986). The platy structure is also commonly observed in aeolian sands (Margolis and Krinsley, 1971; Wellendorf and Krinsley, 1980). Kaldi et al. (1978) experimentally produced such textures by wind abrasion on individual grains from different environments in only 24 h. V-shaped pits arranged in series and other impact marks on a scale of 2–20 μm indicate that all colliding particles were of about the same (small) size. The abundance of these marks further suggests that wind abrasion occurred continuously over a fairly long period. We suggest that beach sands were gradually reworked into coastal dunes.

The third textural group (III) indicates a time of quiescence during which chemical solution left etching pits on the grain surfaces. The establishment of algae on the grains hints at a subaqueous, possibly stagnant environment and a pH ≤ 9 (Krinsley and Margolis, 1969; Coch and Krinsley, 1971). A back-beach with the occasional development of stagnant pools after major storms is a possible environment, although a coastal lagoon cannot be discarded. Le Roux and Elgueta (1997) described barrier island–lagoon complexes along this coastline in the Eocene Trihueco Formation.

The fractures and breakages of the fourth textural group (IV) are linked to a high-energy, probably short-lived event. The

pattern of this group resembles that of a highly turbulent river, shallow marine environment, or mass flow (Higgs, 1979). Conchoidal fractures, for example, are common on glacial grains due to crushing, but this process also occurs during bedload transport by high-energy streams (Trewin, 1988).

4.2. Interpretation of associated features

4.2.1. Ring-shaped structures

The ring-shaped structures in the mudstone underlying the sandstone unit probably represent fluid escape pipes. Although some of these structures superficially resemble hummocky cross-bedding, the latter is unlikely to have developed in such fine-grained sediments.

4.2.2. Sandstone intrusions

Small sandstone dykes protruding downward from debris flow beds have been interpreted by Le Roux et al. (2004) as resulting from cracks produced in the substrate by the seismic shattering of an earthquake, which are subsequently injected by backflow debris before annealing can occur. However, the scale of the Ranquil dykes, as well as the fact that they penetrate the substrate in different directions, requires a different explanation. This aspect is discussed in more detail in Section 5.

Mimic sedimentary structures such as cross-lamination and inverse grading may correspond to the "swirly texture" described in debris flows by some authors (e.g. Amy et al., 2005). However, Peterson (1968) also described structures resembling graded bedding, cross-bedding, ripple marks, flute casts and groove casts in a dyke swarm in Sacramento Valley, California, which he interpreted as laminar, viscous flow structures. In the Ranquil Formation these structures, as well as larger-scale, well developed laminae or beds produced by coarser and finer bands within sills, probably result from dispersive pressures caused by the shearing action within the dense, highly pressurized injections. The orientation of mudstone clasts parallel to the dyke and sill walls is similarly attributed to shearing.

4.2.3. Mudstone-clast breccia

The mudstone clasts and megaclasts were evidently ripped up from the substrate, as they are lithologically similar to the latter, have the same gastropod species in common, and also contain *Thalassinoides* traces. Rip-up probably occurred when sand injected from the overlying flow exploited cracks in the substrate, widened them and finally separated the blocks, as documented by Le Roux et al. (2004) on a much smaller scale in the Coquimbo Formation of north-central Chile.

The mudstone-clast breccia developed when large rafts being transported within the debris flow were broken up by continuing sand injections around their rims (Fig. 16). The break-up process can be deduced from several outcrops where sandstone veins protrude from the surrounding source bed into mudstone rafts and in among already fragmented mudrock clasts. Similar mudstone-clast breccias associated with large-scale sandstone injections have been described by Duranti and Hurst (2004). These authors attributed the fabric of sand filling micro- and larger cracks to hydraulic fracturing (Delaney et al., 1986; Cosgrove, 2001), where high pore fluid pressure reduced the shear strength of the sediments and induced failure.

5. Discussion

5.1. A probable tsunami origin

An important clue as to the origin of the Huenteguapi sandstone lies in the aeolian environment reflected by its grain surface textures, which excludes local cliff failure as the main mechanism generating the debris flow. Coastal dunes cannot collapse on a scale large enough to produce a gigantic mass flow reaching the continental slope, but dune, beach and back-beach sands can easily be swept out to sea by a mega-tsunami flooding and eroding the coastline. This would explain the environmental disequilibrium of the Huenteguapi deposit (which contains coastal fauna within a continental shelf to slope environment) and its unusual thickness, as coastal dunes or barrier island complexes would be able to provide large amounts of easily erodible sand. However, local rocky shoreline taxa in the Huenteguapi sandstone also indicate the existence of coastal outcrops or cobble beaches at some localities.

A tsunami backflow redistributing dune sands over the continental shelf is compatible with the fourth group of grain surface textures, which indicates that a high-energy, turbulent flow was the last event to affect the sediments. A tsunami origin is furthermore supported by the lateral extent of the Huenteguapi sandstone. Debris flows originating from slope collapse are commonly limited to a fairly narrow zone downslope of the point of failure and show abrupt lateral pinchouts (Aksu and Hiscott, 1989; Laberg and Vorren, 1995; Marr et al., 2001). The Huenteguapi sandstone, by contrast, has a continuous width of at least 3 km and probably more than 40 km parallel to the inferred shoreline in the east, as could be expected in the case of a tsunami flooding large parts of the coastline.

Although the Huenteguapi sandstone is never completely exposed so that its maximum thickness is unknown, it must represent an extraordinarily large tsunami event. Tsunami deposits are generally less than 3 m thick (Minoura and Nakaya, 1991; Shiki and Tamazaki, 1996; Massari and D´Alessandro, 2000) and Hartley et al. (2001) considered the 7–10 m thick, Plio-Pleistocene tsunami bed at Hornitos north of Antofagasta as possibly the thickest ever recorded. The maximum exposed thickness of 30 m of the Huenteguapi sandstone is therefore exceptional.

The possibility that the Huenteguapi sandstone can be correlated with the Hornitos deposit can also not be excluded, in which case this would certainly indicate an extraordinary event affecting at least 1600 km of coastline. Partial melting of some quartz grains in the Huenteguapi sandstone suggests impact with very high-energy particles (Mahaney, 2002), which together with the presence of glass particles (tektites?) could support a possible link with an asteroid impact. Felton and Crook (2003) speculated that the Hornitos deposit may be related to the Eltanin bolide, which fell in the region of the Bellinghausen Sea at 2.15 Ma (Gersonde et al., 1997; Ward and

Asphaug, 2002). However, without more precise dating of the Huenteguapi and Hornitos deposits this remains uncertain.

5.2. Origin of sandstone dykes

Sandstone dykes emanating from the base of tsunami beds seldom exceed a meter or two in length (Le Roux et al., 2004; Le Roux and Vargas, 2005). A large-scale dyke complex similar to the Ranquil occurrence has been described from Greenland (Surlyk and Noe-Nygaard, 2003), where downward-injected, ptygmatically folded dykes penetrate underlying mudstones. Interesting enough, the source sand in this case was also deposited by hyperconcentrated density flows.

The timing of the sand injection at Ranquil can be derived from field relationships. Post-burial compaction followed by seismic shattering, as proposed by Surlyk and Noe-Nygaard (2003) for the Greenland complex, can probably be ruled out as the mechanism of intrusion. The injections at Ranquil not only penetrate downward but also horizontally to form sills, from where secondary dykes in turn protrude upward into the overlying muds (Fig. 11), which means that the pressure distribution within the upper part of the substrate must have been fairly homogeneous. If a post-compaction, upward pressure gradient existed, the dykes would have intruded the unit above the Huenteguapi sand and not the substrate (Jolly and Lonergan, 2002). This suggests that the mudstone unit was located at or near the surface and not at depth when the injection took place. The fact that some dykes show ptygmatic folds also supports the notion that burial and compaction occurred after their intrusion.

There is ample evidence that some tensile strength existed within the muddy substrate when clast rip-up occurred. Mudstone blocks as large as 5 m in diameter could not be incorporated into the flow if this were not the case, whereas sand intrusion in the form of dykes and sills would also not take place in a soft, muddy substrate. According to Lowe (1975), Nichols (1995) and Jolly and Lonergan (2002) muds have low cohesion close to the surface and generally fail by plastic deformation and density inversions leading to soft-sediment mixing instead of tabular intrusions. Cohesion may have been produced in the muddy substrate of the Huentegupai sand by the loss of pore fluids prior to or during the tsunami backflow, as supported by the observed fluid escape structures. However, it is not clear whether this was the result of seismic shattering because of a bolide impact, or some other process not presently understood.

Because the cohesive clasts must have been plucked up from the substrate during the tsunami backflow and were in turn injected by sand from within the flow (Fig. 10), the pore pressure within the clasts and by inference in the substrate, must have been lower than in the flow itself. This suggests that a downward pressure gradient existed between the flow and the substrate, which can explain the intrusion of dykes and sills into the latter. The forceful nature of the intrusion is indicated by shear-laminae parallel to the walls of dykes and sills and the inverse size-grading of mudstone clasts. That passive filling of open cracks can be excluded, is also indicated by the presence of sills with dykes protruding upward from them (Fig. 11). Le Roux et al. (2004) suggested that clast rip-up can actually be assisted by small-scale injections from the base of debris flows.

In summary, although the mechanism of sand intrusion at Ranquil is not yet fully understood, it seems clear that there was a loss of fluids from the substrate muds prior to or during the early stages of the flow, producing some tensile strength that allowed large clasts to be plucked up and incorporated into the debris. This fluid loss caused a lower static pressure within the substrate as well as within the mudstone clasts, allowing them to be injected by sand from the debris flow.

5.3. Implications for hydrocarbon exploration

The existence of coarse-grained, extensive sandstone beds within continental slope mudstones has important implications for hydrocarbon exploration. Injected sandstones comprise significant hydrocarbon reservoirs in deep-water systems of the North Sea (Dixon et al., 1995; Bergslien, 2002; Purvis et al., 2002; Hurst et al., 2003) and are also associated with hydrocarbon reservoirs in the Niger Delta (Davies, 2003) and the Norwegian Sea (Møller et al., 2001). Such potential reservoirs may be fed with hydrocarbons along the dykes emanating from their bases, as similar dykes intruding overlying beds have been demonstrated to serve as conduits for oil migration through shale (Jenkins, 1930).

An important aspect is that large sills can resemble sandstone "beds" and can have secondary dykes also penetrating the overlying mudstones, which in borehole cores might lead to the erroneous conclusion that they are older than the latter. They may thus be misinterpreted as deep-water sands remobilized after deposition of the overlying muds. In other cases, dykes may be erroneously considered to have been injected from an unknown, underlying source bed, so that horizontal drilling may be misdirected. Furthermore, the misidentification of mimic sedimentary structures and size-grading of clasts, which may be confused with sedimentary stratification, can lead to erroneous palaeoenvironmental interpretations. This may be exacerbated by having to work with borehole cores or tadpole plots. Deep-water tsunami beds may also contain contemporaneous or older, shallow water micro- and macrofossils eroded from shoreline exposures during the onrush phase, causing further environmental misinterpretation.

The fact that many sandstone dykes of unknown source occur in deep-water, tectonically active settings (Jolly and Lonergan, 2002; Duranti and Hurst, 2004), suggests that some of these structures may have had a similar origin. In the Paleogene succession of the North Sea, mudstone clast-rich sandstones have mostly been interpreted as debris flow deposits (O´Conner and Walker, 1993; Shanmugam et al., 1995; Cullen et al., 1997; Pickering et al., 1997; Jones et al., 2003). However, an alternative interpretation has attributed them to sand injection and associated brecciation (Anderton, 1997; Pickering et al., 1997; Lonergan et al., 2000; Purvis et al., 2002). These apparently contradicting interpretations may have important consequences in predicting the geometry and organization of deep-water sandstones (Duranti and Hurst, 2004). The sandstone dykes and sills at Ranquil show that such large-scale intrusions and associated breccia can indeed result from debris flows, but in this case probably related to tsunami events. Such deposits can cover extensive areas parallel to the shoreline in deep-water environments and may constitute important hydrocarbon reservoirs, in contrast to normal debris

flows that are roughly lenticular and tend to be restricted to channels or submarine canyons perpendicular to the shoreline.

Acknowledgements

This study was funded by Project Fondecyt 1010691 and Deutsche Forschungsgemeinschaft grant Ni699/4-1, which are gratefully acknowledged. Part of this paper was written while JPLR held a Fellowship at the Hanse Institute for Advanced Study in Delmenhorst, Germany. Anne Felton, Keith Crook and two anonymous reviewers suggested many improvements to the text, while Andrew Hurst made sure that some of the more controversial ideas were eliminated. Petrysia Le Roux is thanked for assisting with field work.

References

Aksu, A.E., Hiscott, R.N., 1989. Slides and debris flows on the high-latitude continental slopes of Baffin-bay. Geology 17, 885–888.

Amy, L.A., Talling, P.J., Peakall, J., Wynn, R.B., Arzola Thynne, R.G., 2005. Bed geometry used to test recognition criteria of turbidites and (sandy) debrites. Sedimentary Geology 179, 163–174.

Anderton, R., 1997. Sedimentation and basin evolution in the Paleogene of the Northern North Sea. In: Oakman, C.D., Corbett, P.W.M. (Eds.), Cores from the Northwest European Hydrocarbon Province. The Geological Society of London, pp. 39–47.

Bergslien, D., 2002. Balder and Jotun — two sides of the same coin? A comparison of two Tertiary oil fields in the Norwegian North Sea. Petroleum Geoscience 8, 349–363.

Brown, J.E., 1973. Depositional histories of sand grains from surface textures. Nature 242, 396–398.

Buatois, L., Mángano, M.G., Aceñolaza, F.G., 2002. Trazas Fósiles: Señales de Comportamiento en el Registro Estratigráfico. Museo Paleontológico Egidio Feruglio, Chubut, Argentina. 382 pp.

Bull, P.A., 1981. Environmental reconstruction by scanning electron microscopy. Progress in Physical Geography 5, 368–397.

Cantalamessa, G., Di Celma, C., 2005. Sedimentary features of tsunami backwash deposits in a shallow marine Miocene setting, Mejillones Peninsula, northern Chile. Sedimentary Geology 178, 259–273.

Coch, N.K., Krinsley, D.H., 1971. Comparison of stratigraphic and electron microscopic studies in Virginia Pleistocene sediments. Journal of Geology 79, 426–437.

Cosgrove, J.W., 2001. Hydraulic fracturing during the formation and deformation of a basin: a factor in the dewatering of low-permeability sediments. American Association of Petroleum Geology Bulletin 85, 737–748.

Cullen, B., Ward, B.J., Warrander, J.M., 1997. Facies of the Forties Member in the Nelson Field, UKCS North Sea. In: Oakman, C.D., Corbett, P.W.M. (Eds.), Cores from the Northwest European Hydrocarbon Province. The Geological Society of London, London, pp. 155–174.

Culver, S.J., Bull, P.A., Campbell, S., Shakesby, R.A., Whalley, W.B., 1983. Environmental discrimination based on quartz grain surface textures: a statistical investigation. Sedimentology 30, 129–136.

Davies, R.J., 2003. Kilometer-scale fluidization structures formed during early burial of a deepwater slope channel on the Niger Delta. Geology 31, 949–952.

Delaney, P.T., Pollard, D.D., Ziony, J.I., McKee, E.H., 1986. Field relations between dikes and joints: emplacement processes and paleostress analysis. Journal of Geophysical Research 91, 4920–4938.

Dixon, R.J., Schofield, K., Anderton, R., Reynolds, A.D., Alexander, R.W.S., Williams, M.C., Davies, K.G., 1995. Sandstone diapirism and clastic intrusion in the Tertiary sub-marine fans of the Bruce-Beryl Embayment, Quadrant 9, UKCS. In: Hartley, A.J., Prosser, D.J.U. (Eds.), Characterization of Deep Marine Clastic Systems. Special Publication, 94. Geological Society of London, pp. 77–94.

Duranti, D., Hurst, A., 2004. Fluidization and injection in the deep-water sandstones of the Eocene Alba Formation (UK North Sea). Sedimentology 51, 503–530.

Encinas, A., Maksaev, V., Pinto, L., Le Roux, J.P., Munizaga, F., Zentilli, M., 2006a. Pliocene lahar deposits in the Coastal Cordillera of central Chile: implications for uplift, avalanche deposits and porphyry copper systems in the Main Andean Cordillera. Journal of South American Earth Sciences 20, 369–381.

Encinas, A., Le Roux, J.P., Buatois, L.A., Nielsen, S.N., Finger, K.L., Fourtanier, E., Lavenu, A., 2006b. Nuevo esquema estratigráfico para los depósitos mio-pliocenos del área de Navidad (33°00'-34°30'S), Chile central. Revista Geológica de Chile 33, 221–246.

Felton, E.A., Crook, K.A.W., 2003. Evaluating the impacts of huge waves on rocky shorelines: an essay review of the book 'Tsunami — the underrated hazard'. Marine Geology 197, 1–12.

Finger, K.L., Nielsen, S.N., DeVries, T.J., Encinas, A., Peterson, D.E., 2007. Paleontologic evidence for sedimentary displacement in Neogene Forearc Basins of Central Chile. Palaios 22, 3–16.

García, F., 1968. Estratigrafía del Terciario de Chile central. In: Cecioni, G. (Ed.), Symposio Terciario de Chile, Zona Central. Editorial Andrés Bello, Santiago, pp. 25–58.

Gersonde, R., Kyte, F.T., Bleil, U., Diekmann, B., Flores, J.A., Gohl, K., Grahl, G., Hagan, R., Kuhn, G., Sierro, F.J., Voelker, D., Abelmann, A., Bostwick, J.A., 1997. Geological record of the late Pliocene impact of the Eltanin asteroid in the Southern Ocean. Nature 390, 357–363.

Hartley, A., Howell, J., Mather, M.E., Chong, G., 2001. A possible Plio-Pleistocene tsunami deposit, Hornitos, northern Chile. Revista Geológica de Chile 28, 117–125.

Henriquez, A., 2006. Variaciones locales del nivel del mar en las cuencas neógenas de Caldera, III Región y Arauco, VIII Región: deducción de tasas de alzamiento y subsidencia tectónica. Unpubl. Masters Thesis, University of Chile, Santiago, 170 pp.

Higgs, R., 1979. Quartz surface features of Mesozoic–Cenozoic sands from Labrador and Western Greenland continental margins. Journal of Sedimentary Petrology 49, 599–610.

Hurst, A., Cartwright, J.A., Duranti, D., 2003. Fluidization structures produced by upward injection of sand through a sealing lithology. In: Van Rensburg, P., Hills, R.R., Maltman, A.J., Morley, C.K. (Eds.), Subsurface Sediment Mobilisation. Special Publication, 216. Geological Society of London, pp. 123–137.

Jenkins, O.P., 1930. Sandstone dykes as conduits for oil migration through shales. American Association of Petroleum Geologists Bulletin 14, 411–421.

Jolly, R.J.H., Lonergan, L., 2002. Mechanisms and controls on the formation of sand intrusions. Journal of the Geological Society of London 159, 605–617.

Jones, E., Jones, B., Ebdon, C., Ewen, D., Milner, P., Plankett, J., Hudson, G., Slater, P., 2003. Eocene. In: Evans, D., Graham, C., Armour, A., Bathurst, P. (Eds.), The Millenium Atlas, Petroleum Geology of the Central and Northern North Sea. The Geological Society of London, pp. 261–277.

Kaldi, J., Krinsley, D.J., Lawson, D., 1978. Experimentally produced aeolian surface textures on quartz sand grains from various environments. In: Whalley, W.B. (Ed.), Scanning Electron Microscopy in the Study of Sediments. Geological Abstracts, pp. 261–277. Norwich.

Krinsley, D.H., Donahue, J., 1968. Environmental interpretation of sand grain surface textures by electron microscopy. Bulletin of the Geological Society of America 79, 743–748.

Krinsley, D.H., Margolis, S.V., 1969. Scanning electron microscopy: a new method for studying sand grain surface textures. Transactions of the New York Academy of Science 31, 457–477.

Krinsley, D.H., Doornkamp, J.C., 1973. Atlas of Quartz Sand Surface Textures. Cambridge University Press.

Krinsley, D.H., Wellendorf, W., 1980. Wind velocities determined from the surface textures of sand grains. Nature 283, 372–373.

Krischev, K.G., Georgiev, V.M., 1981. Surface textures of quartz grains as a source of information on sedimentation environment in the South Bulgarian Black Sea shelf. Geologica Balcanica 11, 77–99.

Kulikov, E.A., Rabinovich, A.B., Thomson, R.E., 2005. Estimation of tsunami risk for the coasts of Peru and northern Chile. Natural Hazards 35, 185–209.

Laberg, J.S., Vorren, T.O., 1995. Late Weichselian submarine debris flow deposits on the Bear Island trough-mouth fan. Marine Geology 127, 45–72.

Le Roux, J.P., Elgueta, S., 1997. Paralic parasequences associated with Eocene sea-level oscillations in an active margin setting: Trihueco Formation of the Arauco Basin, Chile. Sedimentary Geology 110, 257–276.

Le Roux, J.P., Elgueta, S., 2000. Sedimentologic development of a Late Oligocene–Miocene forearc embayment, Valdivia Basin Complex, southern Chile. Sedimentary Geology 130, 27–44.

Le Roux, J.P., Vargas, G., 2005. Hydraulic behaviour of tsunami backflows: Insights from their modern and ancient deposits. Environmental Geology 49, 65–75.

Le Roux, J.P., Gómez, C., Fenner, J., Middleton, H., 2004. Sedimentological processes in a scarp-controlled rocky shoreline to upper continental slope environment, as revealed by unusual sedimentary features in the Neogene Coquimbo Formation, north-central Chile. Sedimentary Geology 165, 67–92.

Le Roux, J.P., Gómez, C.A., Olivares, D.M., Middleton, H., 2005a. Determining the Neogene behavior of the Nazca Plate by geohistory analysis. Geology 33, 165–168.

Le Roux, J.P., Gómez, C., Venegas, C., Fenner, J., Middleton, H., Marchant, M., Buchbinder, B., Frassinetti, D., Marquardt, C., Gregory-Wodzicki, K.M., Lavenu, A., 2005b. Neogene-Quaternary coastal and offshore sedimentation in north-central Chile: record of sea level changes and implications for Andean tectonism. Journal of South American Earth Sciences 19, 83–98.

Le Roux, J.P., Olivares, D.M., Nielsen, S.N., Smith, N.D., Middleton, H., Fenner, J., Ishman, S.E., 2006. Bay sedimentation as controlled by regional crustal behaviour, local tectonics and eustatic sea-level changes: Coquimbo Formation (Miocene–Pliocene), Bay of Tongoy, central Chile. Sedimentary Geology 184, 133–153.

Le Roux, J.P., Nielsen, S.N., Henriquez, A., submitted for publication. Depositional environment of *Stelloglyphus llicoensis* isp. nov.: a new radial trace fossil from the Neogene Ranquil Formation (Messinian – Zanclean), south-central Chile. Revista Geológica de Chile.

Linde, K., Mycielska-Dowgiallo, E., 1980. Some experimentally produced microtextures on grain surfaces of quartz sand. Geografiska Annaler, Series A 62 (3-4), 171–184.

Lonergan, L., Lee, N., Johnson, H.D., Jolly, R.J.H., Cartwright, J.A., 2000. Remobilization and injection in deepwater depositional systems: implications for reservoir architecture and prediction. In: Wiemer, P., Slatt, R.M., Coleman, J. (Eds.), Deep-water Reservoirs of the World. GCSSEPM Foundation 20th Annual Bob Perkins Research Conference, pp. 515–532.

Lowe, D.R., 1975. Water escape structures in coarse-grained sediments. Sedimentology 23, 157–204.

Mahaney, W.C., 2002. Atlas of Sand Grain Surface Textures and Applications. Oxford University Press, New York. 237 pp.

Margolis, S.V., Krinsley, D.H., 1971. Submicroscopic frosting on eolian and subaqueous quartz sand grains. Geological Society of America Bulletin 82, 3395–3406.

Marr, J.G., Harff, P.A., Shanmugam, G., Parker, G., 2001. Experiments on subaqueous sandy gravity flows: the role of clay and water content in the flow dynamics and depositional structures. Bulletin of the Geological Society of America 113, 1377–1386.

Martínez, R., 1976. Hallazgo de *Sphaeroidinella dehiscens dehiscens* (Parker and Jones) en el Plioceno de Arauco: su significado para la reinterpretación del Neoceno superior en Chile. Actas I Congreso Geológico Chileno, pp. C125–C142.

Massari, F., D´Alessandro, A., 2000. Tsunami-related scour-and-drape undulations in Middle Pliocene restricted-bay carbonate deposits (Salento, south Italy). Sedimentary Geology 135, 265–281.

Minoura, K., Nakaya, S., 1991. Traces of tsunami preserved in inter-tidal, lacustrine and marsh deposits: some examples from northeast Japan. Journal of Geology 99, 265–287.

Møller, N.K., Kjaernes, P.A., Martinsen, O.J., Charnock, M.A., 2001. Remobilised sands at the Cretaceous/Tertiary boundary in the Ormen Lange Field, offshore mid-Norway. Subsurface Sediment Mobilisation Conference, Abstract Volume, September 2001, p. 13. Gent, Belgium.

Nichols, R.J., 1995. The liquefaction and remobilization of sandy sediments. In: Hartley, A.J., Prosser, D.J. (Eds.), Characterization of Deep Marine Clastic Systems. Special Publication, 94. Geological Society of London, pp. 63–76.

Nielsen, S.N., submitted for publication. Neogene species of *Fissurella* (Gastropoda: Vetigastropoda) from Chile: extending the record of *Fissurella* s.s. back into the early Miocene. The Nautilus.

Nielsen, S.N., 2004. The genus *Olivancillaria* (Gastropoda, Olividae) in the Miocene of Chile: rediscovery of a senior synonym and description of a new species. The Nautilus 118, 88–92.

Nielsen, S.N., Glodny, J., 2006. The middle Miocene climate optimum in central and southern Chile: $^{87}Sr/^{86}Sr$ isotope stratigraphy on warm-water mollusks. XI Congreso Geológico Chileno, Antofagasta, Chile, Actas 2, 93–96.

Nielsen, S.N., Frassinetti, D., Bandel, K., 2004. Miocene Vetigastropoda and Neritimorpha (Mollusca, Gastropoda) of Central Chile. Journal of South American Earth Sciences 17, 73–88.

O´Conner, S.J., Walker, D., 1993. Paleogene reservoirs of the Everest trend. In: Parker, J.R. (Ed.), Petroleum Geology of Northwest Europe, Proceedings of the 4th Conference. The Geological Society of London, pp. 145–160.

Paskoff, R., 1991. Likely occurrence of a mega-tsunami in the middle Pleistocene, near Coquimbo, Chile. Revista Geológica de Chile 18, 87–91.

Peterson, G.L., 1968. Flow structures in sandstone dikes. Sedimentary Geology 2, 177–190.

Pickering, K.T., Vining, B.A., Ioannides, N.S., 1997. Core photograph-based study of stratigraphic relationships of some Tertiary deep-marine lowstand depositional systems in the central North Sea. In: Oakman, C.D., Corbett, P.W.M. (Eds.), Cores from the Northwest European Hydrocarbon Province. The Geological Society of London, pp. 49–65.

Pineda, V., 1983. Evolución paleogeográfica de la Península de Arauco durante el Cretácico Superior- Terciario. Tesis de Grado, Universidad de Concepción.

Pineda, V., 1986. Evolución paleogeográfica de la cuenca sedimentaria cretácico-terciaria de Arauco. In: Frutos, J., Oyarzún, R., Pincheira, M. (Eds.), Geología y Recursos Minerales de Chile, pp. 375–390.

Purvis, K., Kao, J., Flanagan, K., Henderson, J., Duranti, D., 2002. Complex reservoir geometries in deep water clastic sequence, Gryphon Field, UKCS: injection structures, geological modelling and reservoir simulation. Marine and Petroleum Geology 19, 161–179.

Schöning, M., Bandel, K., 2004. A diverse assemblage of fossil hardwood from the Upper Tertiary (Miocene?) of the Arauco Peninsula, Chile. Journal of South American Earth Sciences 17, 59–71.

Shanmugam, G., 2000. 50 years of the turbidite paradigm (1950s–1990s): deep-water processes and facies models–a critical perspective. Marine and Petroleum Geology 17, 285–342.

Shanmugam, G., Bloch, R.B., Mitchell, S.M., Beamish, G.W.J., Hodgkinson, R.J., Damuth, J.E., Straume, T., Syvertsen, S.E., Shields, K.E., 1995. Basin-floor fans in the North Sea — sequence stratigraphic models vs. sedimentary facies. American Association of Petroleum Geologists Bulletin 79, 477–512.

Shiki, T., Yamazaki, T., 1996. Tsunami-induced conglomerates in Miocene upper bathial deposits, Chita Peninsula, central Japan. Sedimentary Geology 104, 175–188.

Surlyk, F., Noe-Nygaard, N., 2003. A giant sand-injection complex: the Upper Jurassic Hareelv Formation of East Greenland. Geologia Croatica 56, 69–81.

Todd, S.P., 1989. Stream-driven, high-density gravelly traction carpets: possible deposits in the Trabeg Conglomerate Formation, SW Ireland and some theoretical considerations of their origin. Sedimentology 36, 513–530.

Trewin, N., 1988. Use of the scanning electron microscope in sedimentology. In: Tucker, M. (Ed.), Techniques in Sedimentology. Blackwell Scientific Publications, Oxford, pp. 229–273.

Ward, S.N., Asphaug, E., 2002. Impact tsunami — Eltanin. Deep-Sea Research II (49), 1073–1079.

Wellendorf, W., Krinsley, D., 1980. The relation between crystallography of quartz and upturned aeolian cleavage plates. Sedimentology 27, 447–453.

Whalley, W.B., Marshall, J.R., 1986. Simulation of aeolian quartz grain surface textures: some scanning electron microscopic observations. In: Sieveking Hart (Ed.), The Scientific Study of Flint and Chert. Cambridge University Press, Cambridge, pp. 227–233.

Whalley, W.B., Marshall, J.R., Smith, B.J., 1982. The origin of desert loess: some experimental observations. Nature 300, 433–435.